

Figure 18 Bending moment distribution in upper beam at  $\theta = \pm 1/200$

Figure 19 Strain distribution in composite beam at  $\theta = \pm 1/200$

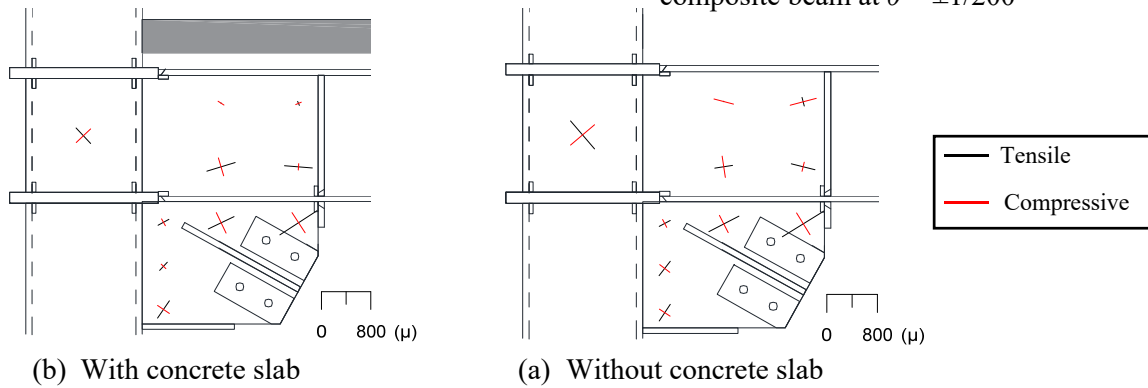


Figure 20 Principal strain distributions at  $\theta = \pm 1/200$

Figure 20 shows the magnitude and direction of the principal strain around the gusset plate in the first cycle of  $\theta = +1/200$ . The principal strain of the gusset plate does not differ with the presence or absence of the concrete slab. The beam moment on the cross section with a gusset plate of the subassembly with the concrete slab was about 1.3 times larger than that of the subassembly without the concrete slab (Figure 18). However, such a result was obtained because strain was less likely to occur due to an increase in cross-sectional performance owing to the presence of the slab.

#### 4. Results of Constant Cycle Loading Tests

Figure 21 shows the relationship between  $Q_f$  and the number of cycles during constant cycle loading. The circled numbers in Figure 21 indicate the order in which the members were damaged. Figure 22 shows the condition of each damaged member. Hereafter, only the subassembly with the concrete slab is described. It was confirmed that  $Q_f$  gradually decreased during both positive and negative loading. It was visually confirmed that local buckling occurred in the beam web from the first cycle, and it is considered that this progressed and  $Q_f$  decreased. At the 9th cycle, the core material of the damper broke (①), and the  $Q_f$  increased accordingly (Eq. 1a) to reach the maximum yield strength. Immediately after that, a crack was formed in the lower flange on the left end of the lower beam. This crack became larger as the loading progressed, and the lower flange fractured (②) at the 13th cycle. After that, the crack progressed to the web and  $Q_f$  decreased gradually. Finally, at the 49th cycle, the lower flange near the gusset end of the upper beam broke (③), and then at the 55th cycle, the  $Q_f$  reached half of the maximum value. With respect to the subassembly without the concrete slab, each fracture property was confirmed with a number of cycles similar to that of the specimen with the slab (① = 12th, ② = 19th, ③ = 58th cycle).

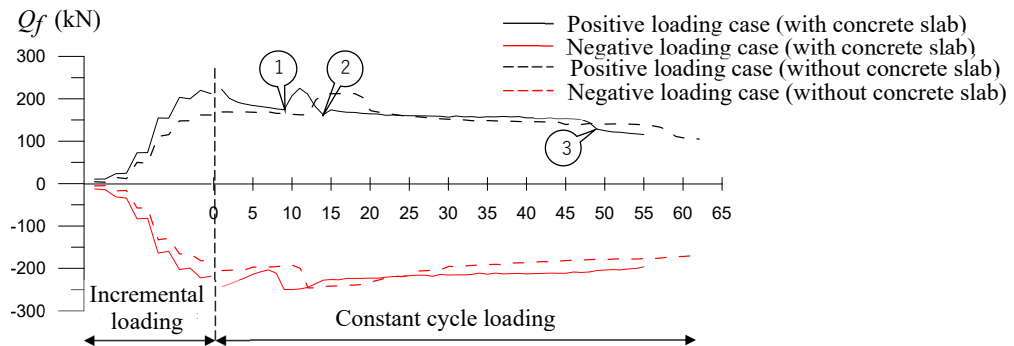
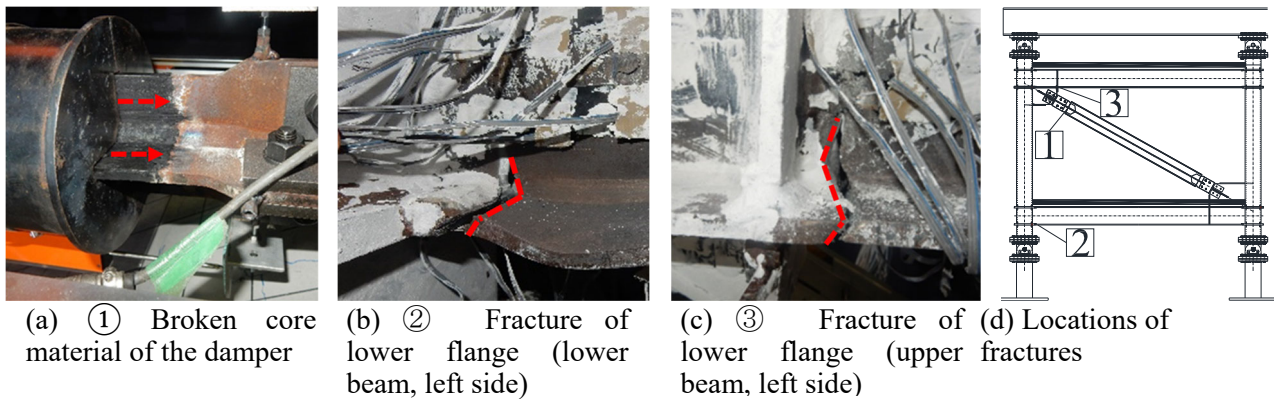
Figure 21 Relationship between  $Q_f$  and number of cycles

Figure 22 Condition of each fracture

## 5. Conclusions

The following conclusions were obtained from the tests of the two subassemblies:

1. It was confirmed that the concrete slab increased the stiffness and strength of the beam in the subassembly. In contrast, the damper behaviors were the same with and without the concrete slab.
2. The energy absorption of the beam increased after the cycle of  $\theta = \pm 1/100$ . Compared to the absorbed hysteretic energy of the damper, it was almost the same during the cycle of  $\theta = \pm 1/50$  and 1.2 to 1.3 times higher in the cycle of  $\theta = \pm 1/33$ .
3. Around the lower gusset plate, the concrete slab and the vertical side stiffener are not in contact with each other, so that bearing pressure from the vertical side stiffener cannot be expected. Therefore, in this vicinity, the strain of the concrete slab directly on the beam web was almost zero, and the effective width was calculated to be short.
4. The subassembly with the concrete slab produced a larger beam bending moment than the subassembly without the concrete slab, but the principal strains on the gusset plates and bottom flange of steel beams were the same as in the subassembly without the concrete slab. This is because strain is less likely to occur due to an increase in cross-sectional performance owing to the presence of the concrete slab. For the same reason, strain in the gusset plates of the subassembly with the concrete slab had the same value as in the subassembly without the concrete slab.



5. In both subassemblies, the core of the damper broke first, then the lower flange on the left end of the lower beam cracked, and finally the lower flange on the left end of the upper beam cracked, leading to failure.

## References

- [1] Kasai, K., Baba, Y., Nishizawa, K., Hikino, T., Ito, H., Ooki, Y., Motoyui (2012): Test results for building with steel dampers, 3D shake table tests on full scale 5-story steel building with dampers Part2. *J. Struct. Constr. Eng.*, No.673, pp. 499-508
- [2] Architecture Institute of Japan (2010). Design Recommendations for Composite Constructions.
- [3] Kasai, K., Watanabe, Y., Minato, N. (2005): Study on dynamic behavior of a passive system with visco-plastic Damper. *J. Struct. Constr. Eng.*, No.588, pp. 87-94
- [4] Kasai, K., Matsuda, Y., Motoyui, S., Kishiki S. (2015): Fundamental Study using New Test Loading Scheme for Steel Frame Subassembly with Damper Connection Details. *J. Struct. Constr. Eng.*, No.708, pp. 309-319
- [5] Yamanobe, K., Yabe, Y., Wada, A. (1996): Lateral loading test on steel frames with 3-spanned continuous composite beams. *J. Struct. Constr. Eng.*, No.487, pp. 121-129
- [6] Matsuda, Y., Kasai, K., Sakai, S., Motoyui, S. (2016): Basic Study on Behavior of Composite Beam Subjected to Double Curvature Bending. *J. Struct. Constr. Eng.*, No.722, pp. 791-801
- [7] M.N. Newmark et.al. (1951): Test and analysis of composite beams with incomplete interaction, Proc. Of the Society of Experimental Analysis, Vol.9, no.1